Defense Technical Information Center Compilation Part Notice

ADP010517

TITLE: Design and Optimization of Wings in Subsonic and Transonic Regime

DISTRIBUTION: Approved for public release, distribution unlimited

This paper is part of the following report:

TITLE: Aerodynamic Design and Optimisation of Flight Vehicles in a Concurrent Multi-Disciplinary Environment [la Conception et l'optimisation aerodynamiques des vehicules aeriens dans un environnement pluridisciplinaire et simultane]

To order the complete compilation report, use: ADA388284

The following component part numbers comprise the compilation report:

ADP010499 thru ADP010530

Design and Optimization of Wings in Subsonic and Transonic Regime

Fernando Monge *, José Jiménez-Varona †
Instituto Nacional de Técnica Aeroespacial (INTA)
Carretera de Ajalvir km 4.5 28850 Torrejón de Ardoz (Madrid), Spain

* Director, Fluid Dynamics Department, e-mail: mongef@inta.es
† Research Engineer, Fluid Dynamics Department, e-mail: jimenezj@inta.es

For a realistic and practical aerodynamic optimization the most appropriate combination of the three sets of tools taking part in the process should be carefully studied. That is, the optimization should allow an easy implementation of constraints, and should be multipoint without the need to prescribe pressure distributions in the objective function; the design space should be broad enough; and the analysis tool should be fast and robust. Taking into account these criteria, a code for multipoint design and optimization of wings in subsonic and transonic regime has been developed and will be described in this paper. The objective can be any combination of the global aerodynamic coefficients, and geometrical and physical constraints can be applied. Results for subsonic and transonic cases will be presented. Flexibility in the use of the design variables allows many different tests to be performed before the best solution is achieved. Lastly, the computational cost is reduced by the use of a low level code for computing the aerodynamic coefficients.

1 Introduction

The quality of the results in the use of numerical optimization for the design of aerodynamic configurations depends on the appropriate choice of a lot of parameters. These are usually interdependent and do not always affect the solution in the same direction, especially when the gradient computation is required. For example, the use of more complex models for computing the flow does not necessarily improve the results because of the numerical noise; this also applies to the type and number of design variables; as well as the way in which the global aerodynamic coefficients are determined, whether by local or far field methods, among many other factors.

The first decision to be taken concerns the type and number of design variables, which is a subject that has not been sufficiently covered in our opinion. The design space should be broad enough to avoid the dependency of the starting geometry in the final solution as much as possible. As a first step we have found it is very important to replace the set of points usually defining the initial geometry by an analytical definition. For that purpose, an automatic adjustment by Bèzier polynomia has been used. After the validation with a data base of many different airfoils it was concluded that at least 25 control points are required to have an an error of definition less than 0.01%, which seems a reasonable criteria if the recommended initial changes in the design variables are 0.001. However, the shape functions originally included in the code (Wagner, Hicks-Vanderplaats, Legendre, etc ...) are still available for comparison purposes.

As regards the CFD codes to be used for computing the objective function robustness is their most essential characteristic for using them in an optimization loop, so that their sensitivity to the numerical data can be kept as low as possible. For this reason, and not only for the computing time, it is convenient to use low level codes as long as the nature of the flow allows us to do so, and particularly if the objective is a function of the global aerodynamic coefficients and, almost in any case, when we are in the first stages of the optimization, far from the final solution.

For the optimization itself a finite differences based commercial code [1] has been used with the options of following the steepest descent or conjugate gradients to where we have added the option of using a quasi-Newton method [2].

These three sets of numerical tools have been combined in a modular way to develop an optimization code for airfoils with high lift devices (*OPTPER*) and another one for wings (*OPTWIN*) that were employed for the application cases to be described in this report. They allow us to choose among different CFD codes ranging from velocity potential coupled with boundary layer until Navier-Stokes (2D) and until full potential coupled with boundary layer (3D). The objective function can be any combination of the global aerodynamic coefficients, and the equality or inequality restrictions to be imposed can be geometrical (leading edge radius, trailing edge angle, maximum thickness, camber, etc...) or physical (pitching moment coefficient, minimum pressure, etc...). Also we profited from the expertise collected in data bases such as ESDU for checking some other constraints like the maximum lift coefficient or the highest adverse pressure gradient along the optimization process.

2 Optimization procedure

The main code has been developed in a modular form in order to allow easy improvement or modification of any of its elements.

In general a geometry exists that requires aerodynamical improvement at certain flow conditions, but it is also possible to start the computation from any wing section selected from a given data base of airfoils, which always gives a kind of a guarantee that the final solution does not depend much on the initial wing. Its planform can also be optimized during the minimization process, but it is mainly designed using structural or handling qualities reasons.

Next the objective function has to be specified. It can be

Paper presented at the RTO AVT Symposium on "Aerodynamic Design and Optimisation of Flight Vehicles in a Concurrent Multi-Disciplinary Environment", held in Ottawa, Canada, 18-21 October 1999, and published in RTO MP-35.

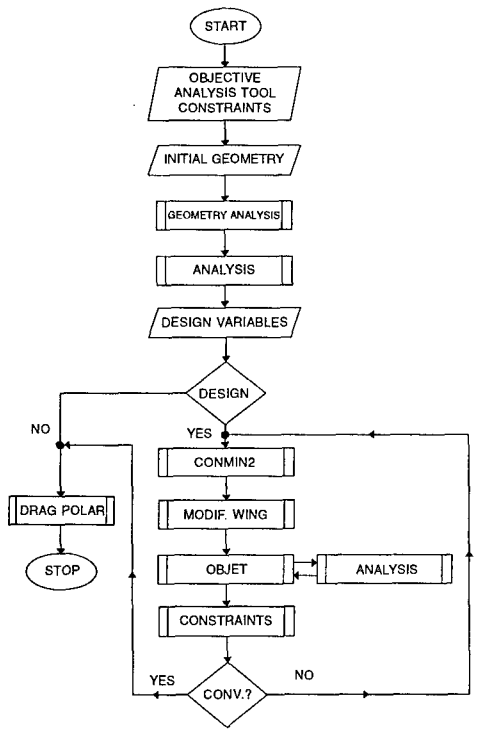

Figure 1: Flow chart for the aerodynamic optimization procedure

any combination of the global aerodynamic coefficients at one or several points of the drag polar. Apart from this, a pressure distribution can be prescribed as objective, but for this purpose the inverse methods are generally more efficient.

Caryying out an exclusively aerodynamic optimization other disciplines are not taken into account (structures, etc...). Generally it is also necessary to impose geometrical and/or physical constraints. At present it is possible to prescribe limits in the wing section area, leading edge radius, angles of thickness and camber line at the trailing edge, thickness at a given positions along the chord, minimum lift, maximum drag, absolute value of pitching moment and maximum velocity. This is also important in order to avoid unfeasible geometries, which is always a risk when the design space is sufficiently large.

For computing the objective function several analysis codes can be selected. In this report a 3D full potential method coupled with an integral boundary layer method has been used. It will be described in the following chapters along with the design variables.

As a minimization tool the original CONMIN code coupled with a BFGS routine to accelerate the convergence has been implemented (CONMIN2).

As regard as the data input, it was distributed in the following way: flow conditions and objective values, initial geometry, numerical parameters of the analysis, numerical parameters of the optimization, and number and type of design variables.

Before the minimization process starts the user may improve the initial geometry by distributing, smoothing and interpolating the original points if there are numerical oscillations in the curvature, which is internally evaluated.

Lastly, the following information can be obtained from the output: final geometry, evolution of design variables, aerodynamic coefficients and objective function. As the new geometry is recorded at the end of every iteration, the user may stop the computation at any time without loosing the previous results, from which a new design strategy may start. In order to verify the quality of the final design a drag polar is computed at the end, and compared with that of the original geometry. The procedure described above is illustrated in figure 1.

3 Design variables

Concerning the design variables different possibilities have been included. First, a set of shape functions to be added to the original wing section was used: Wagner, Hicks-Vanderplaats, Legendre, cubic patches, etc ... After several trials the following functions were chosen [3]:

- *Thickness*

$$f_t(x) = 4 \cdot x^{p(x_{m_i})} \left(1 - x^{p(x_{m_i})}\right) \qquad (1)$$

being $p(x_{m_i})$

$$p(x_{m_i}) = \frac{\log\left(\frac{1}{2}\right)}{\log\left(x_{m_i}\right)} \quad 0 \leq x_{m_i} \leq 1 \qquad (2)$$

and x_{m_i} is the percentage of chord where the maximum of $f_t(x)$ is located.

- *Camber*

$$f_c(x) = 4 \cdot (1-x)^{p(x_{m_i})} \left(1 - (1-x)^{p(x_{m_i})}\right) \qquad (3)$$

being $p(x_{m_i})$

$$p(x_{m_i}) = \frac{\log\left(\frac{1}{2}\right)}{\log\left(1 - x_{m_i}\right)} \quad 0 \leq x_{m_i} \leq \frac{1}{2} \qquad (4)$$

whereas for $\frac{1}{2} \leq x_{m_i} \leq 1$ the expressions 1 and 2 are used.

They provide a more general design space than the other functions, and the number of design variables can be easily increased by an appropriate election of x_{m_i}. An infinite slope at the leading edge for the camber line has been avoided (fig. 2).

In this case we have considered nine design variables in order to control the radius of the leading edge, position and value of the maximum thickness and camber, angle of thickness and camber at the trailing edge, slope of the camber line at the leading edge and with at least one more degree of freedom.

However, when described as usual by a set of coordinates the numerical uncertainties in the definition of the original airfoil can have a negative effect in the optimization. It seems convenient to have the airfoil itself defined from the begining by analytical functions, and not only by the deformation shape functions. To this end a method for fitting the airfoil to a set of Bèzier polynomia has been developed and implemented into the code [4]. The control points are then used as design variables.
One function is used for each upper and lower side of the airfoil, where at the leading edge the continuity of first and second derivatives is imposed:

$$Y_{u,l}(s) = \sum_{i=0}^{NB} Y_{u,l}^{B} \binom{NB}{i} s^i (1-s)^{NB-i} \qquad (5)$$

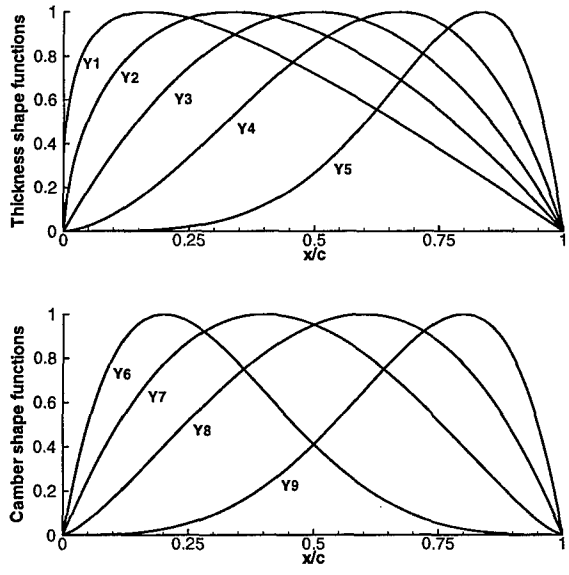

Figure 2: Thickness and camber shape functions

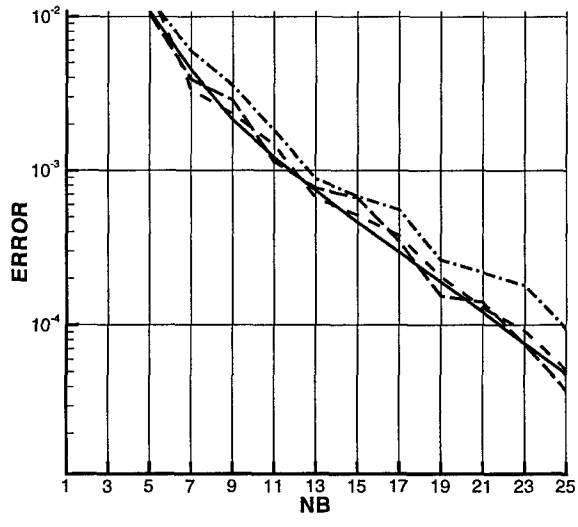

Figure 3: Bèzier fitting error for different airfoils

being Y the fitted coordinates, NB the number of Bèzier control points, s ranges between $0,\ldots,1$. The subscripts u and l denote upper and lower side respectively, whilst the superscript B means the Bèzier control point coordinates.
By solving two least square problems the control points $Y^B_{u,l}$ are computed. This can be done by numerical optimization or by directly solving the system of algebraic equations:

$$[A_{ij}]\{Y^B\} = \{B_{Y_i}\} \quad i,j = 1,\ldots,NB-1 \qquad (6)$$

where,

$$A_{ij} = \sum_{k=1}^{NP}\left[\binom{NB}{i}\binom{NB}{j} s_k^{i+j}(1-s_k)^{2NB-(i+j)}\right] \qquad (7)$$

and,

$$B_{Y_i} = \sum_{k=1}^{NP}\left[\binom{NB}{i} s_k^i(1-s_k)^{NB-i}\cdot(y_0(s_k) - y_0(s_1)(1-s_k)^{NB} - y_0(s_{NP})s_k^{NB})\right] \qquad (8)$$

NP is the number of points defining the wing section and y_0 are the coordinates of the original wing sections.

We have used this last approach not only because of the much lower computing time required but also and mainly because not so many numerical parameters are required as in the first method.

Once the problem is posed and the solution method developed the main question is about the most appropriate number of control points for defining the airfoil and its deformations in order to have a large enough design space. A set of very different airfoils has been tested (conventional, laminar, supercritical, high-lift, etc...) and the outcome is that if the average error needs to be less than 10^{-4}, around 25 control points are required (fig 3). If an error of 10^{-3} is admissible then only 13 control points are needed. These errors are measured 1.0 being the chord of the airfoil. The results have been checked by using different solution methods: Gauss-Jordan, Cholesky and QR.

We must also mention that, in any case, given to the nature of matrix $[A_{ij}]$, there are no additional benefits in using more than 30 control points due to numerical errors.

As a main conclusion, the use of 25 control points is recommended, which represents in general 21 design variables by taking into account the boundary conditions at the leading and trailing edges. This value is much higher than those mostly used up to now, but we consider it necessary for the solution to be independent of the design space.

4 Flow solver

The flow solver utilized in the present code for 3-D computations is the *FLO22vis* (INTA version). This code employs a viscous-inviscid interaction method in a direct iterative way to compute the flow past swept wings in transonic regime. It is based on the inviscid solver FLO22 by Jameson and Caughey [5] and the integral boundary layer code BL3D by Stock [6], recently modified by Yang and Wichmann at DLR [7]. The inviscid solver FLO22 has been modified at INTA to render the trailing edge as a grid line [8]. Additionally, the coupling procedure and the smoothing techniques for the displacement thickness have been improved. A more detailed explanation follows.

4.1 *Inviscid solver*

The inviscid solver is a finite differences code which solves the full potential equation in its non-conservative form in a non orthogonal co-ordinate system. The co-ordinate system is generated by a sequence of transformations. In its original formulation, the spanwise co-ordinate lines were aligned with the leading edge, but cut across the trailing edge in a tapered wing. In order to render the trailing edge as a grid line, an additional scaling by the local wing chord has been introduced in each of the wing sections. In the resulting co-ordinate system, both the leading and trailing edges are grid lines. New stretching transformations have been used outside the wing to increase the distance of the far field to the wing and to better implement the boundary conditions. The stretch-

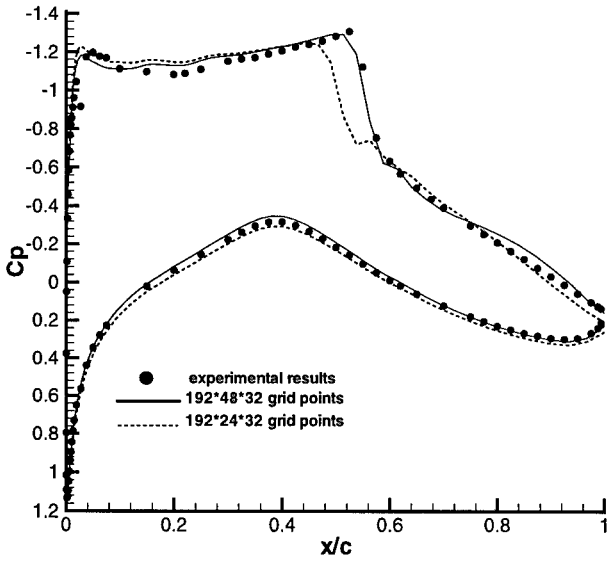

Figure 4: RAE 2822 airfoil. Cp distribution at $M = 0.73$, $Re = 6.5 \cdot 10^6$ and $CL = 0.8$

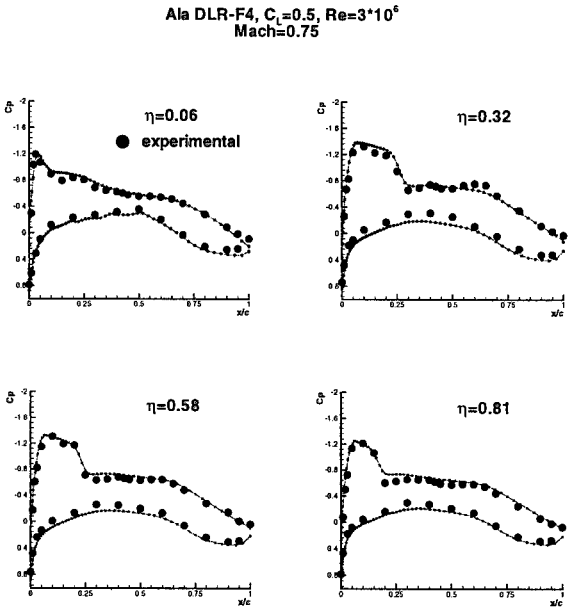

Figure 5: DLR F4 wing. Cp distributions on several spanwise sections at $M = 0.75$, $Re = 3 \cdot 10^6$ and $C_L = 0.5$

ing in normal direction at transonic flow is especially important. The resultant system of non linear algebraic equation is solved by an iterative relaxation procedure SLOR (Successive Line Over Relaxation).

4.2 *Viscous solver*

The viscous solver is an integral boundary layer code. It solves the laminar and turbulent boundary layers in a general non-orthogonal curvilinear coordinate system. In the laminar part, a family of similarity profiles of Falkner-Skan is used in the streamwise direction, whilst a combination of these profiles are used in crossflow direction. For the turbulent boundary layer, Coles velocity profiles of two parameters are used in the streamwise direction, and Mager or Johnston profiles are used in the crossflow direction. Transition is fixed or is computed by a set of empirical correlations. The $4^{th}-$order Runge-Kutta scheme is used for the numerical integration, in which the x-direction is the marching direction.

4.3 *Coupling procedure*

The concept of displacement thickness is used for the interaction of the external flow with the boundary layer. This method only provides a proper treatment of 'weak interaction' phenomena. An underrelaxation technique is introduced to avoid instabilities, and a special smoothing of the displacement surface by means of cubic Bèzier splines is employed to avoid strong irregularities in the shock region and in the trailing edge.

4.4 *Validation*

The flow solver has been widely validated after its improvement. Two sample cases in transonic flow will be shown below. It is important to compare not only global values but also pressure distributions. For potential flow, isentropic flow and irrotational flow are assumed. Discrepancy with the correct Rankine-Hugoniot result is small if the shock upstream Mach number is $M_1 \leq 1.3$. Moreover, the viscous-inviscid interaction takes into account only weak interaction phenomena. At $M_1 \geq 1.3$ incipient separation occurs, thus our viscous-inviscid coupling is less accurate.

4.4.1 RAE 2822 airfoil

A limit case for comparison may be case 9 of reference [9]. At $M = 0.73$, $Re = 6.5 \cdot 10^6$ and $\alpha = 3.19$ deg. the boundary layer measurements show flow close to separation, and the shock upstream Mach number is $M_1 \approx 1.3$. Figure 4 shows the comparison of experimental and computed pressure distributions. The dashed line shows the result using a grid of $192 \cdot 24 \cdot 32$ points, and the solid line represents the results with a mesh of $192 \cdot 48 \cdot 32$ points. There is an important difference in the shock location. The reason is that, with the stretching transformation used in the normal direction, the far field is too close to the wing with the coarser mesh. A finer grid is needed to have the far field at a sufficient distance to avoid any influence of the far field into the supersonic zone. Although not shown here, the boundary layer parameters show good agreement with the experimental ones before the shock. After the shock, there are some differences, especially in the displacement thickness.

4.4.2 DLR-F4 wing

Another test case of a typical transonic wing will be shown. During 1997-98 INTA has participated in the *AEREA F4 Model Test Programme* to study the scale effects on the DLR-F4 wing-body model in the new criogenic european tunnel *ETW* (European Transonic Windtunnel). The range of Reynolds number was $3 - 33 \cdot 10^6$ and the range of Mach number was $0.6 - 0.81$. Thus, the amount of experimental information is very important and permits the validation and assessment of CFD codes [10, 11]. In this AEREA campaign, pressure measurements were not made, but there are experimental data obtained by the *Garteur Group AG-01* [12]. Figure 5 shows the C_p distribution in several spanwise sections of the DLR-F4 wing at $M = 0.75$, $C_L = 0.5$ and $Re = 3.0 \cdot 10^6$.

The computational mesh used had $192 \cdot 48 \cdot 64$ grid points and the computational time was about $1\frac{1}{2}$ hour in a SGI DN 10000 Power Challenge workstation (300 mflops). The mesh is finer than in the previous case to take into account the large variations of geometry in spanwise direction; otherwise the shock will not be

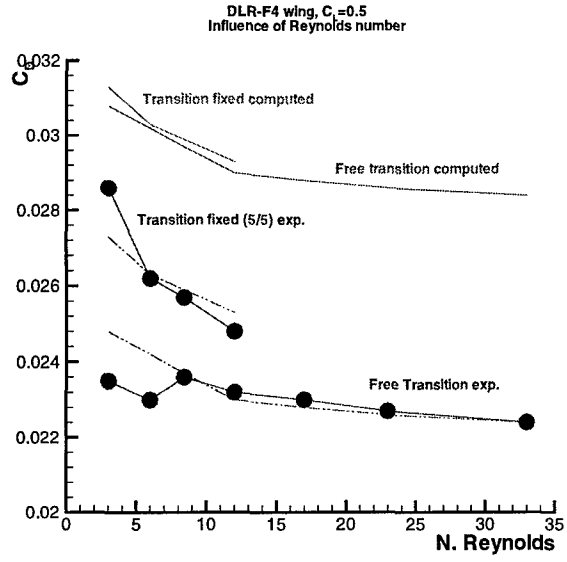

Figure 6: DLR-F4 wing. Reynolds effects on drag coefficient at $C_L = 0.5$

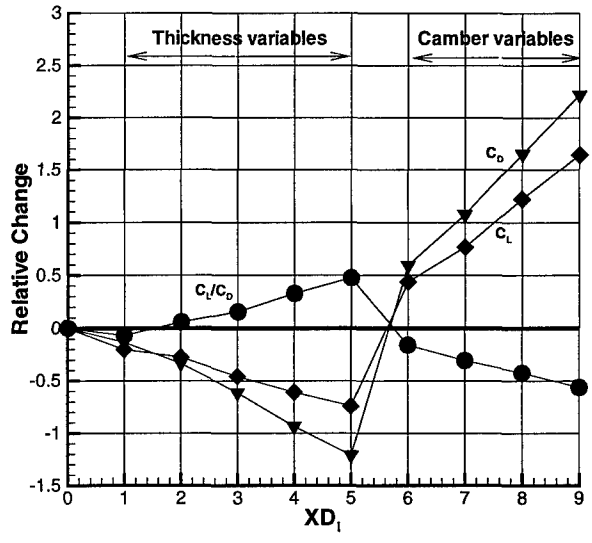

Figure 7: Sensitivity analysis for the subsonic case

properly captured. It can be seen that the comparison of the theoretical results with the experiments is good. There are some differences in the lower side due to the incapability of the flow solver to predict the influence of the body, and also to difficulties in the implementation of Kutta condition.

With regard to global values, figure 6 shows the drag coefficient at $M = 0.785$ and $C_L = 0.5$ at several Reynolds numbers. The comparison is done with fixed transition (5%/5%) and free transition. The fuselage drag has been computed using an analytical procedure. The figure shows that drag is overestimated using the code, but it is worth noting that the experimental results have not been corrected, and that Reynolds number effects include pseudo Reynolds number effects due to aeroelastic distorsion. Two curves representing a translation of the theoretical curves have additionally been plotted in the figure to compare the trends of both theoretical and experimental results. It can be observed that, despite the results at Reynolds number of $3 \cdot 10^6$ for fixed transition and $3 - 6 \cdot 10^6$ for free transition, the influence of Reynolds number in drag is well predicted. It must be underlined that at Reynolds number of $3 \cdot 10^6$ a small trailing edge separation is present in the kink region of the trailing edge [12], thus the drag increases.

A general conclusion is that the code can predict the flow past wings in transonic regime at attached flow conditions with sufficient accuracy. These are the cruising conditions. The advantage of using this kind of code is that an optimization code with this flow solver will not be highly time consuming.

5 Results

To show the capabilities of the method two cases (subsonic and transonic) have been tested. But before any optimization run can be started it is important to take into account several considerations. With the same engineering objective there are many different ways to proceed. For example, the aerodynamic efficiency could be optimized by using it directly as objective function, or by optimizing C_L with C_D as constraint or viceversa. But it is also possible that not all of those three strategies will provide a feasible design, if any.
On the other hand, when viscous effects are included in the analysis the changes in the objective function can be highly non linear and it is very important to choose the most appropriate values for the initial design variables, not so small that the objective does not change, and not so large that the modified geometry can not be analyzed. That's why we have first computed the sensitivities of C_L and C_D to changes in the design variables. It also gives us an idea of the convergence criteria to use in the optimization run in order to avoid as many analyses as possible. Lastly, it provides useful information about the convenience or not for scaling the variables and for applying limiting values.

5.1 *Subsonic case*

The first exercise has been the optimization of the wing of an RPV called *SIVA (Sistema Integrado de Vigilancia Area)* designed at INTA. The flow conditions are $M = 0.2$ and $Re = 1.5 \cdot 10^6$. The wing has no twist, a surface of 4.5 sq.m., 5.81 m of span, 0.905 and 0.485 m of chord at the root and at the tip, respectively. Among a broad set of different airfoils, the *Eppler-580* was selected. At cruise conditions the angle of attack is 1.5 deg. and the lift coefficient $C_L = 0.56$.

By using the nine design variables described in § 3 (eqs. 1 to 4) the sensitivities computed for a change of 10^{-3} in each variable are plotted in fig. 7. There is an slight decrease in lift and drag when the thickness increases, but the efficiency $\left(\frac{CL}{CD}\right)$ in general increases, and more so when the deformation approaches the trailing edge. The opposite happens as regards the camber deformation.

From these values the following problem has been posed: improvement of $\left(\frac{CL}{CD}\right)$ at a weighted rate of 0.5 at 0.0 deg. and 0.5 at 2.0 deg. with the constraint of having a section area not smaller than that of the original one. By running a multipoint optimization, the use of an arbitrary constraint in the leading edge radius is avoided. It is also advisable not to use higher values of angle of attack when the accuracy of the results gets worse. The flow is supposed to be fully turbulent.

A design with the airfoil Eppler-580 as starting geometry was carried out. A sequence of three meshes, from coarse to fine, are utilized in order to accelerate the convergence and to save computing time. The geometry obtained is plotted in fig. 8 compared with the original one. As

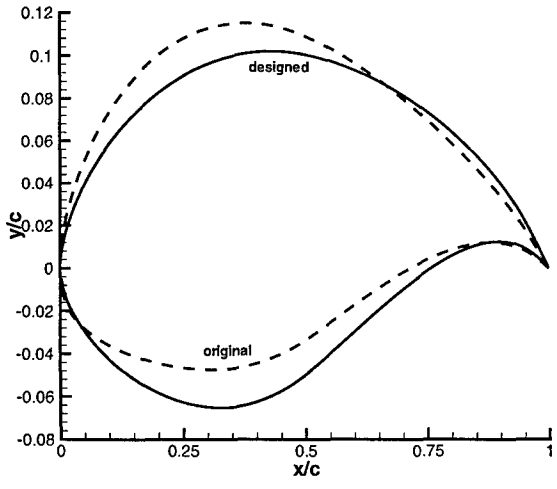

Figure 8: Geometries of both original and designed wing sections for the subsonic case

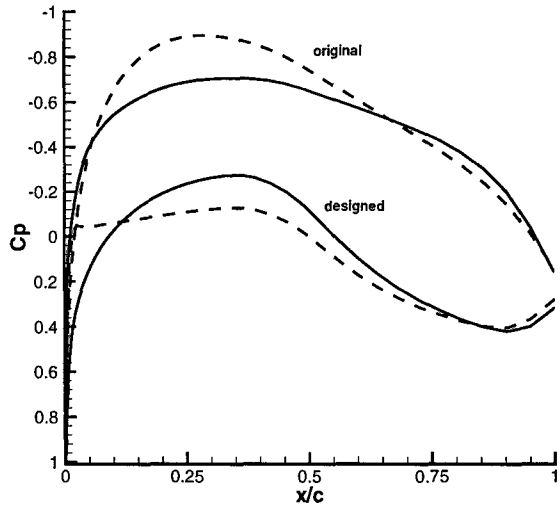

Figure 10: Pressure coefficient at central section of both original and designed wing (subsonic case)

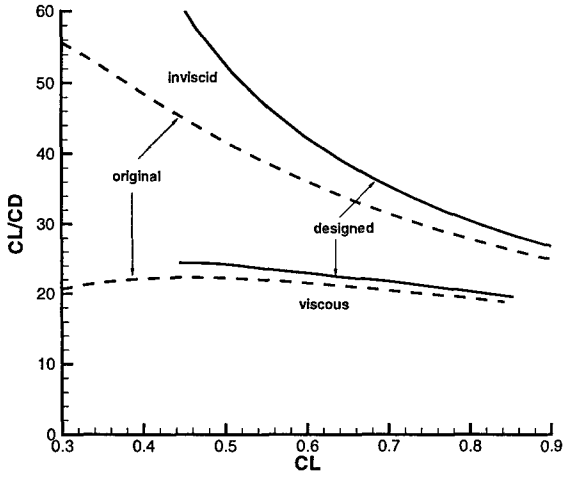

Figure 9: Efficiency vs lift coefficient for the original and designed wing in inviscid and viscous flow (subsonic case)

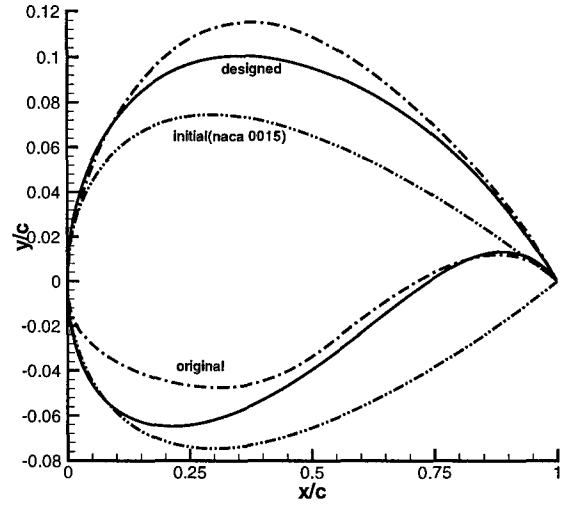

Figure 11: Geometries of NACA 0015, original and designed wing sections for the subsonic case

expected from the sensitivity results the camber has decreased for most of the chord. The efficiencies for a range of $C_L's$ are plotted in fig. 9 where the results for an inviscid run are also included. For the viscous computation the efficiency is improved 9.4%.

The pressure distributions for the mid section of both wings are represented in fig. 10. It can be seen that the maximum velocity has decreased, which is usually positive in terms of drag. Besides, the pressure gradient around the leading edge on the lower side is much smoother. A further study should be made about the more adverse pressure gradient close to the trailing edge on the upper side, using different verification methods.

In order to check the dependency of the solution on the initial geometry an additional design has been carried out with the same objective and constraints as before, but starting from a conventional wing section (NACA-0015). The results are plotted in figures 11 and 12. It can be seen that even in this case the aerodynamic characteristics of the original section have also been improved, showing in a broader sense the capabilities of the method.

Lastly, a test case using Bèzier polynomia has been carried out. It is enough using 13 control points (10 design variables) for an error of 10^{-3}, as it was pointed out in figure 3. A finer grid than in the previous cases has been used. The grid is a C-H mesh of $160 \cdot 24 \cdot 32$ points, fine enough in a subsonic case. The initial wing section is again the NACA 0015 airfoil. The total number of design cycles needed were 8, with 85 evaluations of the objective function. The search direction was that of the BFGS (quasi-Newton) method. Additionally, there is no asumption of fully turbulent flow. The transition is computed by means of empirical methods. The computing time was 24 *hours* 49 *min* in a SGI Power Challenge workstation (300 mflops). Figure 13 shows the initial section, the original section of the *SIVA* wing and the designed section using the Bèzier polynomia. The efficiencies of both the original and designed wing are plotted in figure 14. In order to increase confidence in the new design, two different codes have been used to analyze both the original and designed wings. One code is the solver employed by our

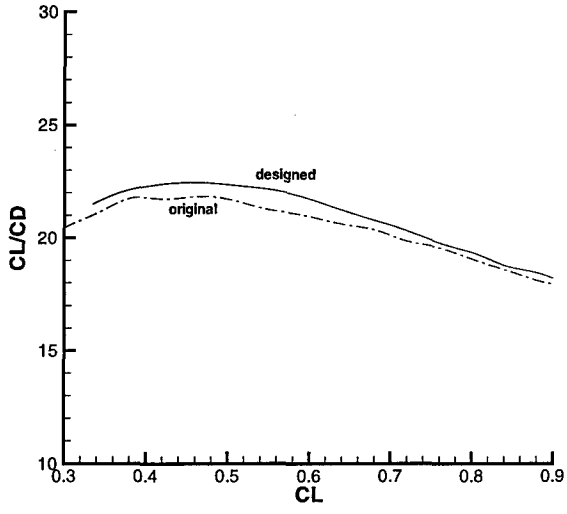

Figure 12: Efficiency vs lift coefficient for the original and designed wing with NACA 0015 as initial section (subsonic case)

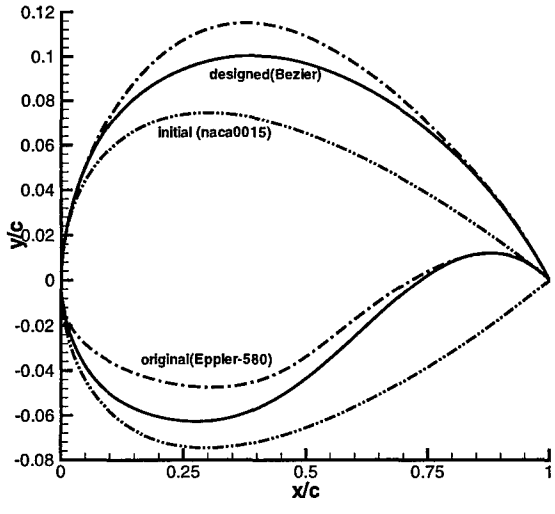

Figure 13: Geometries of NACA 0015, original and designed wing sections for the subsonic case using Bèzier polynomia

optimization method, i.e. *FLO22vis* code, and the other one is a commercial low order panel method coupled to an integral boundary layer method (*VSAERO* code). This code computes a lower drag than the former one, but it is worth noting that both codes show similar trends for both wings. There are some differences in the high C_L values range. In this case the results of the finite differences code are less accurate. In cruise condition both codes predict a similar improvement of the efficiency.

A final comment on this case is that, a design of the wing section of an RPV has been performed starting from an initial section far from the 'optimal' one. The result is an airfoil with similar behaviour of the selected airfoil (Eppler-580) at cruise conditions, and also at off-design conditions. A very few number of constraints have been imposed. This result shows the capabilities of the optimization method presented in this paper. The cost in terms of computational effort is not so high.

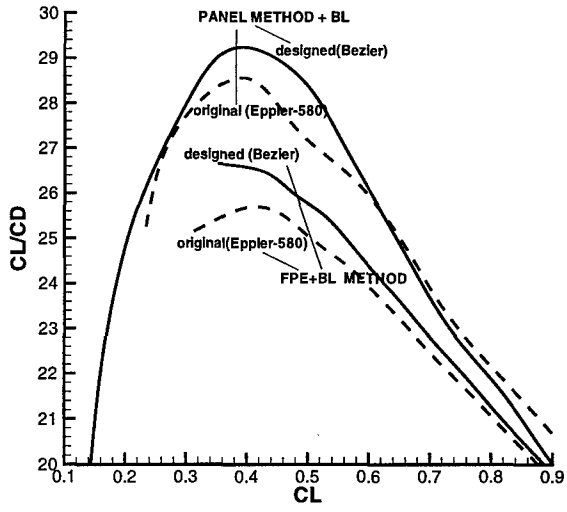

Figure 14: Efficiency vs lift coefficient for the original and designed wing using Bèzier polynomia with NACA 0015 as initial section (subsonic case)

5.2 *Transonic case*

The design of transonic wings is more time consuming than in subsonic flow. In order to simplify the optimization procedure, the design shown in this paper was done fixing the planform and twist, and the wing sections are the same in every spanwise section of the wing. In these conditions, the improvement of wing features will depend on the airfoil features. The wing to improve is a trapezoidal wing of aspect ratio $AR = 8.0$, leading edge sweep angle $\Lambda = 27.5$ deg., taper ratio $\lambda = 0.4$ and linear twist. A typical grid for wing analysis has $192 \cdot 48 \cdot 48$ points. For the optimization, a coarser mesh will be used, because of the computational time. Figure 15 shows the transonic wing.

With the same design variables as used in the subsonic case, the sensitivities are plotted in figs.16,17. This time comparing the inviscid and viscous results.

As shown, the risk of obtaining very different designs when using viscous and inviscid analysis is high, as the sign of the gradients is different for some design variables and aerodynamic coefficients. For instance, by increasing the thickness in the rear part of the wing section the drag also increases when the analysis is inviscid but decreases for a viscous analysis.

The design conditions are $M = 0.82$, $Re = 6.0 \cdot 10^6$. The goal is to improve $\left(\frac{CL}{CD}\right)$ at a weighted rate of 0.5 at 1.5 deg. and 0.5 at 3.0 deg. with the constraint of having a section area not smaller than that of the original one.

The design is done using nine design variables described in § 3 (eqs. 1 to 4). The final wing section can be seen in fig.18 along with the original one. In the same figure the section designed by running the analysis as inviscid is plotted. It is not surprising that in this case the first impression is that the geometry does not look good due to the solution being much more dependent on the design variables used as there is a greater occurence of local minima. The need to take viscous effects into account is clear, especially in transonic flow where the interaction between the shock wave and the boundary layer can so greatly modify the designed geometry.

The efficiencies of the original wing and the viscous design are plotted in fig. 19. As expected in any transonic case, for the final evaluation of both two wings at

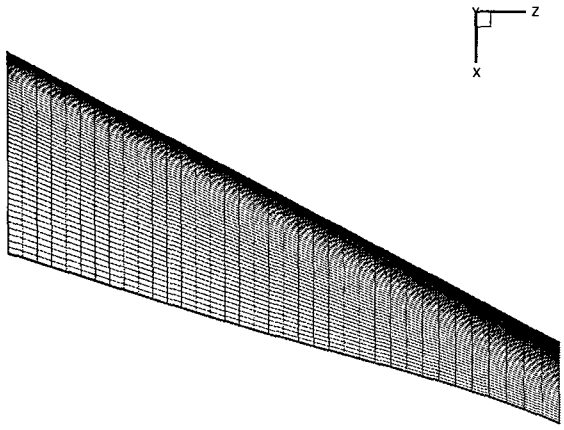

Figure 15: Planform view of the transonic wing. Typical surface mesh for analysis

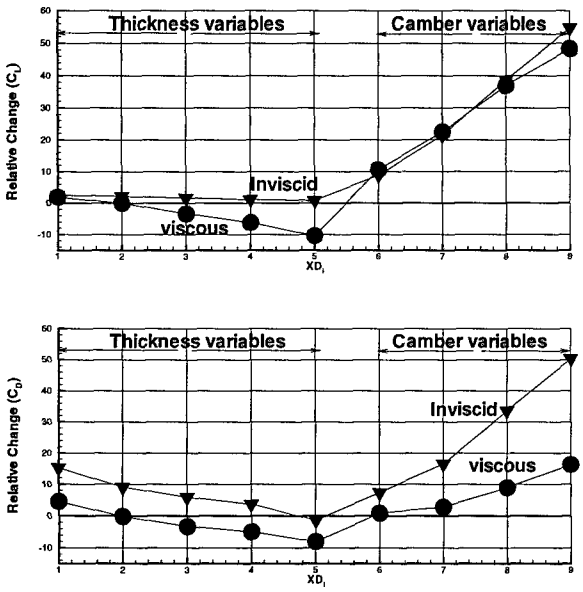

Figure 16: Sensitivity analysis for the transonic case

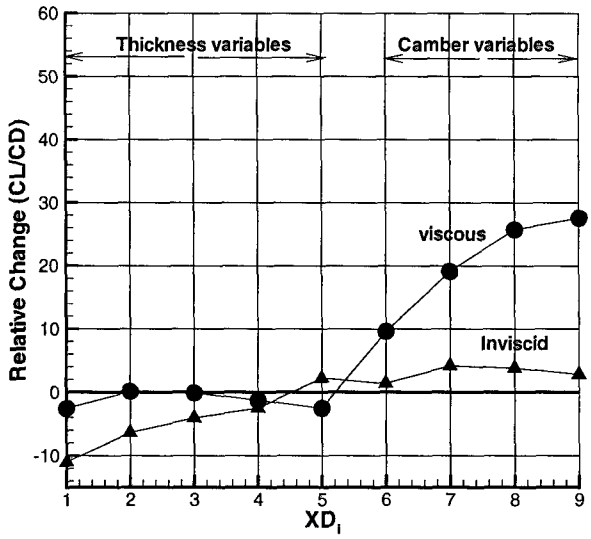

Figure 17: Sensitivity analysis for the transonic case (con't)

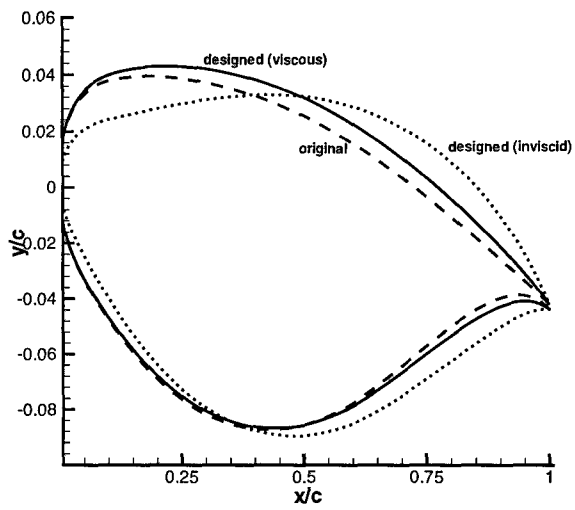

Figure 18: Geometries of both original and designed wing sections for the transonic case

off-design conditions this time it is not so important to include viscous effects compared with the subsonic case (fig. 9) as the relative contribution of friction drag is smaller. At the main design condition the efficiency is improved by 23.5%. As can be seen in fig.20, the main changes in the pressure distribution at the same flow condition are located, as expected, around the shock wave, which is now weaker, while it remains almost the same on the lower surface.

6 Conclusions

A modular optimization code for wings has been described. It allows any combination of the global aerodynamic coefficients to be used as objective function along with a broad set of geometrical and physical constraints. Even though it is possible to use a prescribed pressure distribution as an objective, it is not necessary to know anything about it. The examples shown here have been run on a SGI DN-10000 Power Challenge workstation (300 mflops). In any case, most designs can be obtained from one day to another.

There are many more capabilities than those included in this paper, especially in the selection of the number and type of the design variables, including the planform modification, but the decision will be provided by the application to more different cases. At the moment, the following recommendations can be mentioned:

- From our experience in airfoil design (and we think it can also be extended to wings) it is not clear whether in any of the cases there are advantages in using high level codes instead of low level ones, taking into account that at design conditions the flow is expected to be attached and the shock waves, if any, are weak. Besides, the low level codes are generally more robust.

- On the contrary, care needs to be taken about the size of the design space. It has been shown that unless the changes in the geometry are expected to be small, around thirty design variables for a real wing

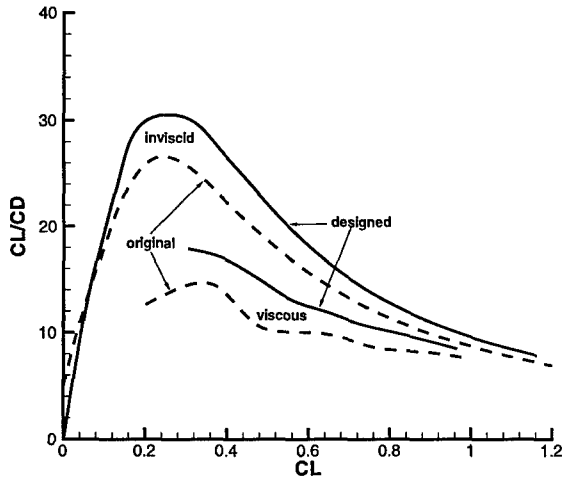

Figure 19: Efficiency vs lift coefficient for the original and designed wing in inviscid and viscous flow (transonic case)

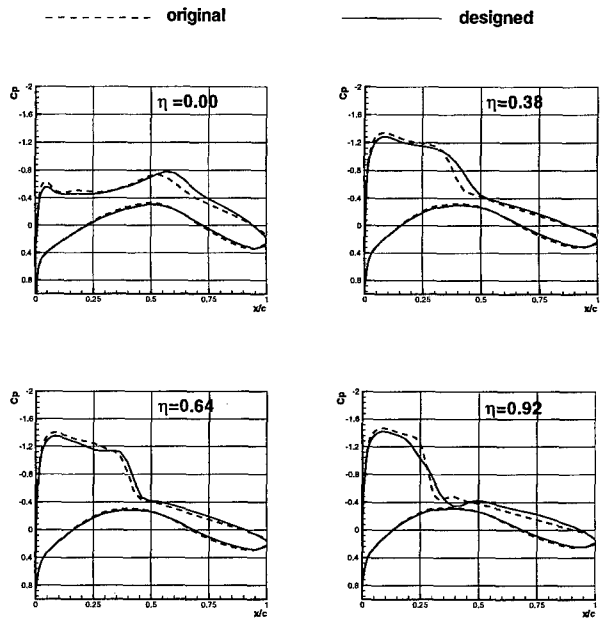

Figure 20: Cp distributions on several spanwise sections at $M = 0.82$, $Re = 6 \cdot 10^6$ and $\alpha = 1.5$ deg. (transonic case)

design are needed, including planform modification.

- There is no engineering design without the possibility of running multipoint optimization.
- Lastly, even though the viscous contribution can be small, in any case the analysis should include viscous effects, especially in the transonic cases when no pressure distribution is prescribed, even if the friction drag is not included in the objective. Otherwise, the final geometry could be unfeasible or at least very dependent of the design variables used.

Finally, in the short term we plan to include the options already available in the 2D code OPTPER mentioned above for the design and optimization of airfoils; namely, to add the option of free transition as a new design variable [13] and to use control theory for computing the gradients [14].

Acknowledgements

The work presented in this paper has been developed and financed by INTA's own research. The authors are grateful to Veronica Watson, who kindly revised this manuscript.

References

[1] G.N. Vanderplaats. CONMIN -a Fortran Program for Constrained Function Minimization, User's Manual. Technical Report TM X-62,282, NASA, 1978.

[2] W. Press, W. Vetterling, S. Taukolsky, and B. Flannery. *Numerical Recipes in FORTRAN, The Art of Scientific Computing.* Cambridge University Press, 1992.

[3] V. Ibañez, F. Monge, and B. Tobío. Estrategias de Diseño Aerodinámico : Métodos Inversos y de Optimización. In 3er *Congreso de Métodos Numéricos en Ingeniería, Zaragoza*, Junio,3-6,1996.

[4] B. Tobío and F. Monge. Optimizacion numérica de perfiles aerodinámicos definidos mediante polinomios de Bézier. In *V Encontro Nacional de Mecanica Computacional, Guimaraes*, October,20-22,1997.

[5] A. Jameson and D.A. Caughey. Numerical Calculation of the Transonic Flow Past a Swept Wing. Contractor Report 153297, June 1977.

[6] H.W. Stock. Integral Method for the Calculation of Three-Dimensional, Laminar and Turbulent Boundary Layers. Technical Report 77/51 B, Dornier, 1978.

[7] Yang Q.-Z. and G. Wichmann. Calculation of Transonic Wing Flow by Interaction of a Potential and an Integral Three Dimensional Laminar-Turbulent Boundary Layer Method. Technical Report IB 129-98/11, DLR, August 1998.

[8] José Jiménez-Varona. Computations of DFVLR-F4 model using a Viscous Flow Solver for Transonic Wings. Technical Report AT/TNO/4510/001/INTA/98, INTA, February 1998.

[9] P.H. Cook, A. McDonald, and M.C.P. Firmin. Aerofoil RAE 2822 - Pressure Distributions, and Boundary Layers Measurements. In *AGARD-AR-138*, pages A6–1 to A6–77, 1979.

[10] D. Schimanski. The AEREA F4 Model Test Campaign. Technical Report E 9004 TR 0009, European Transonic Windtunnel, January 1998.

[11] D. Schimanski. ADDENDUM to TEST REPORT of the AEREA F4 Model Test Campaign. Technical Report E 9004 TR 0012, European Transonic Windtunnel, September 1998.

[12] G. Redeker et al. A Selection of Experimental Test Cases for the Validation of CFD Codes. In *AGARD AR-303*, volume 2, 1994.

[13] F. Monge and G. Vicente. Diseño aerodinámico de perfiles multicomponentes con transición libre. In *V Encontro Nacional de Mecanica Computacional, Guimaraes*, October,20-22,1997.

[14] F. Monge and B. Tobío. Aerodynamic design and optimisation by means of control theory. In *IV World Congress on Computational Mechanics, Buenos Aires, Argentina*, June, 29-July 2,1998.

DISCUSSION

Session III, Paper #21

Dr Nangia (Nangia Aero, UK) suggested that pitching moment should be included in the optimizations, as this would strongly affect Cl/Cd conclusions through the effect on trim drag, etc...

Mr Monge agreed, pointing out that the option to take account of pitching moment as a constraint, or within the object function, is already included in his code. The sample cases presented in the paper were only intended to show some of the tool's capabilities.